

## RESEARCH ARTICLE

# Integrating tracking and resight data enables unbiased inferences about migratory connectivity and winter range survival from archival tags

Clark S. Rushing,<sup>1,2,\*</sup> Aimee M. Van Tatenhove,<sup>1</sup> Andrew Sharp,<sup>1</sup> Viviana Ruiz-Gutierrez,<sup>3</sup> Mary C. Freeman,<sup>4</sup> Paul W. Sykes Jr.,<sup>4</sup> Aaron M. Given,<sup>5</sup> and T. Scott Sillett<sup>2,6</sup>

<sup>1</sup> Department of Wildland Resources and the Ecology Center, Utah State University, Logan, Utah, USA

<sup>2</sup> Smithsonian Migratory Bird Center, National Zoological Park, Washington, District of Columbia, USA

<sup>3</sup> Cornell Lab of Ornithology, Cornell University, Ithaca, New York, USA

<sup>4</sup> U.S. Geological Survey, Patuxent Wildlife Research Center, Warnell School of Forestry and Natural Resources, University of Georgia, Athens, Georgia, USA

<sup>5</sup> Town of Kiawah Island, Kiawah Island, South Carolina, USA

\*Corresponding author: [clark.rushing@usu.edu](mailto:clark.rushing@usu.edu)

Submission Date: September 11, 2020; Editorial Acceptance Date: February 2, 2021; Published April 17, 2021

## ABSTRACT

Archival geolocators have transformed the study of small, migratory organisms but analysis of data from these devices requires bias correction because tags are only recovered from individuals that survive and are re-captured at their tagging location. We show that integrating geocator recovery data and mark–resight data enables unbiased estimates of both migratory connectivity between breeding and nonbreeding populations and region-specific survival probabilities for wintering locations. Using simulations, we first demonstrate that an integrated Bayesian model returns unbiased estimates of transition probabilities between seasonal ranges. We also used simulations to determine how different sampling designs influence the estimability of transition probabilities. We then parameterized the model with tracking data and mark–resight data from declining Painted Bunting (*Passerina ciris*) populations breeding in the eastern United States, hypothesized to be threatened by the illegal pet trade in parts of their Caribbean, nonbreeding range. Consistent with this hypothesis, we found that male buntings wintering in Cuba were 20% less likely to return to the breeding grounds than birds wintering elsewhere in their range. Improving inferences from archival tags through proper data collection and further development of integrated models will advance our understanding of the full annual cycle ecology of migratory species.

**Keywords:** archival tracking tags, integrated Bayesian models, mark–resight data, migratory connectivity, Painted Bunting, *Passerina ciris*, survival bias

## LAY SUMMARY

- Recent advances in the miniaturization of tracking devices have transformed the ability of researchers to track small migratory birds throughout their journeys. However, the small size of these devices prevents transmitting the data to satellites, so birds must be recaptured to obtain the tracking data.
- Because tracking data can only be obtained from individuals that survive and return the following year, these data underestimate how many birds migrate to regions where they are less likely to survive, which may lead to incorrect conclusions about what areas are most important to a species.
- We show that more accurate estimates of migratory patterns can be obtained by combining the data from the tracking tags with information about the survival of individuals within each population.
- Application of this method to tracking data from Painted Buntings revealed that males wintering in Cuba experience nearly 15–20% lower survival than males wintering elsewhere in the range.

## La integración de datos de rastreo y de avistamientos repetidos permite inferencias no sesgadas sobre la conectividad migratoria y la supervivencia en el rango de invierno a partir de marcadores de registro

## RESUMEN

Los geo-localizadores de registro han transformado el estudio de los organismos migratorios pequeños, pero el análisis de los datos provenientes de estos aparatos requiere correcciones de sesgo debido a que los marcadores son solo recuperados de individuos que sobreviven y que son recapturados en su ubicación de marcado. Mostramos que la integración de datos de geo-localizadores recuperados y de marcas-reavistamientos permiten estimaciones no sesgadas

tanto de conectividad migratoria entre poblaciones reproductivas y no reproductivas, como de probabilidades de supervivencia específicas por región para los lugares de invernada. Usando simulaciones, primero demostramos que un modelo bayesiano integrado genera estimaciones no sesgadas de probabilidades de transición entre los rangos estacionales. También usamos simulaciones para determinar cómo diferentes diseños de muestreo influyen la capacidad de estimar las probabilidades de transición. Luego, parametrizamos el modelo con datos de rastreo y datos de marca-reavistamiento de las poblaciones en disminución de *Passerina ciris* que se reproducen en el este de Estados Unidos, hipotéticamente amenazadas por el comercio ilegal de mascotas en partes de su rango no reproductivo del Caribe. De modo consistente con esta hipótesis, encontramos que los machos de *P. ciris* que invernan en Cuba tuvieron un 20% menos de probabilidad de regresar a los sitios reproductivos que las aves que invernarón en otros lugares de su rango. Mejorar las inferencias a partir de los marcadores de registro mediante la colecta adecuada de datos y el subsecuente desarrollo de modelos integrados permitirá avanzar nuestro entendimiento sobre la ecología del ciclo completo anual de las especies migratorias.

**Palabras clave:** conectividad migratoria, datos de marca-reavistamiento, marcadores de rastreo y registro, modelos bayesianos integrados, *Passerina ciris*, sesgo de supervivencia

## INTRODUCTION

Rapid advances and miniaturization of tracking technology in recent decades have allowed researchers to quantify seasonal migrations of many terrestrial and aquatic species (Eckert and Stewart 2001, Domeier and Nasby-Lucas 2013, Jiménez López et al. 2019), to discover previously unknown migration routes (Sawyer et al. 2009, Smith et al. 2014, Naidoo et al. 2016), and to identify critical migration stop-over and nonbreeding areas (Richter and Cumming 2008, Delmore et al. 2012, Cooper et al. 2019). This information is essential for understanding population dynamics, disease transmission, range shifts, resource use, and management of vulnerable migratory species or populations. Relatively large species (>60 g body mass) can be tracked with geolocation tags capable of transmitting location data to satellites (Scarpignato et al. 2016), but mapping seasonal movements and winter quarters for the great majority of migratory vertebrate species requires miniature archival geolocators (hereafter “geolocators”) that store location data internally and must be recovered from surviving individuals (Fraser et al. 2012, Hallworth and Marra 2015, Peterson et al. 2015).

Although geolocators have been revolutionary for the study of small migratory organisms (McKinnon and Love 2018), interpretation of migration patterns from the observed data must be done with care. In particular, because geolocators do not transmit data, observed migration data can only come from individuals that survive multiple migratory and stationary periods, return to their tagging location, and are recaptured. Individuals that do not survive at any other stage of the annual cycle will not be represented. This form of *survivorship bias* is problematic for inferring migration patterns if certain migration routes have lower survival than others. For example, if the nonbreeding range of a migratory species consists of two regions, one with high survival and one with low survival, individuals that migrate to the low-survival region will be less likely to return to their breeding site than individuals

from the high-survival region. Hence, individuals from the low-survival region will be under-represented in the observed data relative to their actual proportion. Estimates of transition probabilities (i.e. the probability that an individual from breeding site *i* migrates to nonbreeding region *j*) will therefore be under-estimated for low-survival regions, and over-estimated for high-survival regions (see Supplemental Material Appendix S1 for additional proof). Despite the potential for this bias to influence inferences from archival geolocators, a cursory review of the literature suggests that quantifying patterns of migratory connectivity based on the interpretation of raw, observed geolocator data is standard practice (McKinnon and Love 2018, Lisovski et al. 2020).

An analogous bias must be accounted for when estimating movement rates from band recoveries or re-sights with geographic variation in recovery/re-sight probabilities (Brownie et al. 1993, Nichols et al. 1995, Cohen et al. 2014). Although a long history of model development is available to estimate these observation probabilities in dead-recovery and live-re-sight studies (reviewed by Korner-Nievergelt et al. 2010), we lack an equivalent approach to account for the effects of survivorship bias in movement studies based on data from geolocators. Survivorship bias is an inevitable outcome of using archival geolocators when survival differs among migration routes and is therefore likely to be pervasive in the published literature.

Here we present an integrated model that accounts for survivorship bias when estimating migratory transitions from geolocators. Our approach is similar to the integrated model proposed by Korner-Nievergelt et al. (2017) in that it formally combines a geolocator recovery model with capture-recapture data in a single, unified model of migratory connectivity. Our approach extends this framework by recognizing that the average survival probability of a migratory population can be parameterized as the marginal survival probability across all possible nonbreeding regions. In other words, the survival probability measured

by capture–mark–recapture (CMR) methods is the average survival of each nonbreeding region weighted by the probability that an individual migrates to each region. As a result, individuals migrating to low-survival regions result in both missing geolocator recoveries and lower survival probability for the population as a whole. An additional benefit of this integrated model is that it provides estimates of regional survival probabilities without the need to collect additional data during the nonbreeding season. Our objectives are twofold. First, we use simulated data to demonstrate that the method is able to return unbiased estimates of transition probabilities and to determine how different sampling designs influence the estimability of transition probabilities. Second, we apply the model to tracking data from Painted Buntings (*Passerina ciris*), a declining migratory songbird that is thought to be threatened by illegal pet trade in parts of its nonbreeding range. The estimated transition probabilities and nonbreeding survival probabilities from our analysis are consistent with predictions about where Painted Buntings are most at risk of capture during the winter, underscoring the potential of these methods to improve inference from geolocators and reveal new insights into the ecology and conservation of migratory species.

## MATERIALS AND METHODS

We assume that researchers deploy archival geolocators to determine migration routes used by different populations of a focal species with an annual cycle consisting of stationary breeding and nonbreeding periods, separated by annual migrations. Delineation of populations will depend on the study system and will often be based on sampling logistics (Cohen et al. 2018), though may also be based on geopolitical boundaries, genetic data (Ruegg et al. 2014), or demographic data (Rushing et al. 2016). Researchers deploy geolocators at  $s = 1, 2, 3, \dots, S$  breeding sites over  $t = 1, 2, 3, \dots, T$  years and each recovered geolocator is used to assign individuals  $i = 1, 2, 3, \dots, I$  to one of  $j = 1, 2, \dots, J$  distinct nonbreeding regions. The objective of the study is to determine the proportion of individuals from breeding site  $s$  that migrate to nonbreeding region  $j$ , which we represent by a  $S \times J$  transition matrix  $\Psi$ . In addition to the deployment of geolocators, we assume that researchers also apply marks (e.g., leg bands) to individuals in each breeding site to estimate apparent annual survival at each of the  $S$  breeding sites using mark–recapture or mark–re-sight methodologies. The integrated model we outline below assumes that geolocator individuals are not included in the mark–capture data set, though small violations of this assumption are unlikely to have practical effects on inference (Abadi et al. 2010).

These data provide the following summaries:

- (1)  $\mathbf{N}$ : a  $S \times T$  matrix containing the number of geolocators deployed at site each breeding site in each year
- (2)  $\mathbf{w}$ : a  $S \times J \times T$  matrix indicating the number of recovered geolocators from site  $s$  that spent the nonbreeding season in region  $j$  in year  $t$
- (3)  $\mathbf{y}_s$ : an  $I \times T$  matrix containing the annual encounter histories of marked birds at site  $s$

For the purposes of this paper, we assume no uncertainty in determining the nonbreeding region of each individual, though it may be possible to relax this assumption (see Discussion). In most applications, survival data will be collected over longer time scales than geolocator data, which should not pose problems as long as the estimated survival probabilities apply to individuals tracked using geolocators.

Both the geolocator data and the mark–recapture data contain information about the underlying transition matrix  $\Psi$ , allowing us to integrate these two data sets within a single analysis. In the sections below, we describe sub-models for the geolocator recovery and mark–recapture data that allow us to parameterize each model in terms of the underlying transition matrix.

### Geolocator Recovery Model

Rather than interpret the  $\mathbf{w}$  entries as proportional to  $\Psi$  (the default of most archival tagging studies), we derive an explicit geolocator recovery model that treats  $\mathbf{w}$  as a random variable governed by both the transition matrix and annual survival probabilities for birds wintering in each nonbreeding region. For each breeding site  $s$  and year  $t$ , we model the observed number of geolocator individuals from breeding site  $s$  that went to nonbreeding region  $j$  as:

$$w_{s,t} \sim \text{multinomial}(\phi \Psi_s P, N_{s,t}) \quad (1)$$

where  $w_{s,t}$  is a vector indicating the number of recovered tags from each nonbreeding region,  $\phi$  is a vector containing the annual apparent survival probabilities for individuals that migrated to each nonbreeding region,  $\Psi_s$  is a vector indicating the probability that a bird from site  $s$  migrates to each nonbreeding region (with the constraint that  $\sum_{j=1}^J \psi_{js} = 1$ ), and  $P$  is the probability of recapturing a geolocator individual given that it survived and returned. For the model described here, we assume that  $P$  is constant across all sites and years, though this assumption could be relaxed by including occasion-specific sampling covariates via a logit-link. We also assume  $\Psi$  and  $\phi$  are constant across years. This assumption could also be relaxed by including covariates (e.g., sex) and/or allowing temporal variation in one or both parameters. Our calculation of  $\phi$  also assumes that mortality can occur anywhere during the annual cycle

(e.g., on fall migration or winter quarters) and is independent of breeding location. Finally, our formulation assumes that geolocator individuals are captured in the year following tag deployment. This will often be the case in many studies, though it is possible for recoveries to occur multiple years after tag deployment. Although we do not show it here, this situation could be incorporated into the model by parameterizing the geolocator recovery model at the individual level and indexing recovery probabilities based on the appropriate number of survival occasions.

### Mark–Recapture Model

Encounter data from marked individuals can be used to estimate the probability that an individual breeding at site  $s$  survives and returns to breed the next year ( $\Phi_s$ ), which is equivalent to the marginal probability of survival across the entire nonbreeding area (i.e. the average nonbreeding survival weighted by the transition probabilities to each region). Apparent survival can be estimated using a variety of capture–recapture methods, for example the standard Cormack–Jolly–Seber (CJS) model:

$$\begin{aligned} z_{i,s,t} &\sim \text{Bernoulli}(\Phi_s z_{i,s,t-1}) \\ y_{i,s,t} &\sim \text{Bernoulli}(d_{s,t} z_{i,s,t}) \end{aligned} \quad (2)$$

where  $z_{i,s,t}$  is the true state (dead or alive) of individual  $i$  in year  $t$  and  $d_{s,t}$  is the probability of detecting an individual given that it is alive and present at site  $s$  in year  $t$ . Again, it is possible to model heterogeneity in these parameters by including covariates on detection probability using a logit-link.

Assuming that the marked and geolocator birds have the same survival probability, overall survival probability at each breeding site is equivalent to the average of the nonbreeding survivals weighted by the proportion of individuals that spent the nonbreeding season in each region:

$$\Phi_s = \sum_{j=1}^J \phi_j \psi_{js} \quad (3)$$

Equation (3) allows us to parameterize the CJS model in terms of the underlying transition matrix  $\Psi$  and regional survival probabilities  $\phi$ , thereby integrating the two sub-models.

### Simulations

We used simulated data to determine what biological scenarios yield unbiased estimates of  $\Psi$  and  $\phi$ . In CMR models, parameter identifiability can be assessed by simulating capture histories for a very large number of individuals and then quantifying the bias of parameter estimates from the model (Gimenez et al. 2004). With large sample

sizes, the observed frequencies should be equal to their expected values (i.e. no sampling error) and thus any bias in the estimated parameters indicates unidentifiable parameters.

### Identifiability of $\Psi$ and $\phi$

To determine whether  $\Psi$  and  $\phi$  are identifiable using the model described by Equations (1–3), we simulated geolocator recovery and CMR data assuming 10,000 geolocators deployed at each of 3 breeding sites and 20,000 new individuals added to the CMR data in each year at each site. These values were chosen to be large enough that estimates of  $\Psi$  and  $\phi$  were not influenced by sampling error (Gimenez et al. 2004). For each breeding site, we simulated random transition probabilities to each of 3 nonbreeding regions by drawing random values from Uniform (0.2,0.9) and then scaling to ensure the transition probabilities summed to 1. Restricting values to 0.2–0.9 ensured that transition probabilities were not close to 0. Transition probabilities for each breeding site were then combined to create the true  $\Psi$  matrix for the simulation. We next simulated a random survival probability for each nonbreeding region by sampling from Uniform(0.2,0.9), which spans realistic annual survival probabilities for small migratory birds (Sæther 1989). Finally, we used Equations (1–3) to generate geolocator recoveries and capture histories using the  $\Psi$  matrix and  $\phi$  vector created in the previous steps. We repeated these steps 500 times to generate a wide range of transition probabilities and survival probabilities. In all simulations, we assumed 5 years of CMR data,  $P = 0.8$  and  $d = 0.6$ .

For each simulated data set, we estimated the joint likelihood of the model using JAGS version 3.3.0 (Plummer 2012) called from program R version 3.6.0 (R Core Team 2016) with package *jagsUI* version 1.4.2 (Kellner 2016). Tag recovery probability  $P$ , detection probability  $d$ , and nonbreeding survival probabilities  $\phi$  were given uninformative Uniform(0,1) priors. Priors for the elements of  $\Psi$  were given uninformative Dirichlet priors to ensure that the rows of  $\Psi$  summed to 1. Capture histories were summarized using the multi-dimensional array format for computational efficiency. For all models, we ran 3 chains for 25,000 iterations each after an adaptation phase of 1,000 iterations and discarding the first 2,000 iterations as burn-in. Convergence was confirmed through Rhat values and visual inspections of trace plots.

Denoting the estimated transition probability from site  $s$  to region  $j$  for the  $i^{\text{th}}$  simulation ( $i \in 1 - 500$ ) as  $\hat{\psi}_{i,s,j}$ , we measured relative bias in the transition estimates to each nonbreeding as  $\frac{1}{5}(\hat{\psi}_{i,s,j} - \psi_{i,s,j})/\psi_{i,s,j}$ . To compare the estimates from the integrated model to the uncorrected estimates from the raw geolocator recoveries, we also converted the elements of  $\mathbf{w}_i$  to proportions and measured



relative bias in the connectivity to each nonbreeding region as  $\frac{1}{S} \sum_{s=1}^S (w_{i,s,j} - \psi_{i,s,j}) / \psi_{i,s,j}$ . We predicted that the uncorrected estimates would be negatively biased for regions with low survival (transition probabilities underestimated) and positively biased for regions with high survival (transition probabilities overestimated) whereas the corrected estimates from the integrated model would be unbiased for all survival estimates. Because “low” and “high” are defined relative to survival probabilities for other nonbreeding regions, we scaled the survival probabilities within each simulation to range from 0 (for the lowest survival region) to 1 (for the highest survival region). To test our prediction about the relationship between bias and nonbreeding survival, we estimated the correlation between bias of each element of  $w_{i,s,j}$  and  $\hat{\psi}_{i,s,j}$  and the corresponding relative survival probabilities. We predicted that the correlation should be positive for the uncorrected estimates and close to 0 for the corrected estimates. Finally, we measured relative bias for each estimate of  $\phi_j$  as

$$\frac{1}{500} \frac{1}{3} \sum_{i=1}^{500} \sum_{j=1}^3 (\hat{\phi}_{i,j} - \phi_{i,j}) / \phi_{i,j}$$

In addition to estimating transition and survival probabilities, many tracking studies are interested in quantifying the strength of migratory connectivity (i.e. the extent to which individuals and populations remain together between seasons of the annual cycle; Cohen et al. 2018). The strength of migratory connectivity, hereafter *MC*, is a function of the transition matrix  $\Psi$ . Estimating *MC* from the uncorrected transition matrix  $\mathbf{w}$  could therefore result in biased estimates. However, *MC* measures the relative links between breeding and nonbreeding populations and may not suffer from survivorship bias if transition probabilities are equally biased for all focal populations (J. Hostetler personal communication). For each simulated data set  $i$ , we used the *calcMC* function from the *MigConnectivity* R package (Hostetler and Hallworth 2018) to estimate *MC* using the “true” transition matrix  $\Psi$  (hereafter  $MC_{\Psi,i}$ ), the raw observation matrix  $\mathbf{w}$  (hereafter  $MC_{w,i}$ ), and the estimated matrix  $\hat{\psi}$  from the integrated model (hereafter  $MC_{\hat{\psi},i}$ ). We measured relative bias in  $MC_{w,i}$  and  $MC_{\hat{\psi},i}$  as  $(MC_{k,i} - MC_{\Psi,i}) / MC_{\Psi,i}$ , where  $k$  equals either  $w$  or  $\hat{\psi}$ , and report the median bias of the 500 simulations.

### Estimability of $\Psi$

Even if  $\Psi$  is intrinsically identifiable, a number of factors may influence whether estimates of transition probabilities are unbiased under real-world sampling scenarios (i.e. whether the parameters are estimable; Auger-Méthé et al. 2016). We conducted 3 simulation scenarios to determine what factors influence the estimability of  $\Psi$ :

**Number of geolocators.** To investigate how the number of deployed geolocators and marks influences the estimability of  $\Psi$ , we simulated data with sample sizes more typical of geocator and CMR studies. Specifically, we simulated data assuming 10, 20, 30, 40, and 50 geolocators deployed at each breeding site and 40, 75, 125, 200, and 300 individuals added to the CMR data set in each year. As in the identifiability simulations, we assumed 3 breeding and 3 nonbreeding sites, 5 years of CMR data,  $P = 0.8$  and  $d = 0.6$ . The number of geolocators and the number of marked individuals were varied in a factorial design, resulting in 25 simulation scenarios. For each scenario, we simulated 500 data sets with randomly generated  $\Psi$  matrices and  $\phi_j$  values.

**Number of years.** The number of years included in the CMR study may influence the estimability of  $\Psi$  by influencing the precision of the  $\Phi_s$  estimates. We simulated data assuming 4, 6, 8, 10, and 12 years of CMR data. As for the other simulations, we generated 500 data sets with random  $\Psi$  matrices and  $\phi_j$  values for each simulation. For all simulations in this scenario, we assumed 3 breeding and 3 nonbreeding sites, 30 geocator deployed at each site, 100 individuals added to the CMR data set in each year,  $P = 0.8$  and  $d = 0.6$ .

**Number of sites.** Increasing or decreasing the number of deployment sites and nonbreeding regions could influence estimability through its influence on the precision of survival and transition probability estimates. We simulated data assuming 3, 4, 5, 6, and 7 breeding sites and nonbreeding regions. We generated 500 data sets with random  $\Psi$  matrices and  $\phi_j$  values for each simulation and we assumed 5 years of CMR data, 30 geolocators deployed at each site, 100 individuals added to the CMR data set in each year,  $P = 0.8$  and  $d = 0.6$ .

For all estimability simulations, model fitting and evaluation was conducted as described above.

### Application to Eastern Painted Bunting Population Data

Painted Buntings are small (~16 g) migratory songbirds that breed in two distinct populations within the United States (Herr et al. 2011). The “western” population breeds primarily in Texas, Oklahoma, Louisiana, and Arkansas while the “eastern” population is restricted to a narrow band of habitat along the coasts of Florida, Georgia, South Carolina, and North Carolina. Monitoring data indicate that the eastern population has declined steadily over the past half-century (Sykes Jr. and Holzman 2005), likely due to habitat loss and the illegal pet trade (Sykes et al. 2007, 2019). Capture of adult males for the pet trade is thought to be a particular problem in Cuba, where keeping wild birds as pets has a long history. However, data on the pet trade are largely anecdotal and the effects of this threat on the

demography of Painted Bunting populations have not been demonstrated (Sykes Jr. et al. 2006).

In 2017 and 2018, we deployed 180 light-level geolocators (model P50Z11-7-DIP, Migrate Technology Ltd, Coton, Cambridge, UK) on adult male Painted Buntings at 6 sites that span the latitudinal distribution of the eastern population: Carolina Beach State Park, North Carolina (34.15°N, 77.88°W), Dewee's Island, South Carolina (32.84°N, 79.72°W), Kiawah Island, South Carolina (32.61°N, 80.15°W), Spring Island, South Carolina (32.33°N, 80.83°W), Little St. Simons, Georgia (31.29°N, 81.34°W), and Little Talbot Island, Florida (30.46°N, 81.42°W). For the purposes of this analysis, we treated the three South Carolina sites as a single population unit due to their close proximity. Buntings were trapped at feeders using mist nets and traps baited with untreated, white proso millet (*Panicum vergi*). Geolocators were attached with a leg-loop harness (Rappole and Tipton 1991). We recovered 65 geolocators in 2018 and 2019; 61 had viable data. Recovery effort was similar among all sites. We used the R package *SGAT* (Lisovski and Hahn 2012) to generate location estimates from the raw light data. Twilights were identified using the function *preprocessLight* from the R package *TwGeos* (Lisovski et al. 2016). We used a light-level threshold of 1 or 2 for all birds, depending on the amount of shading in the data. We used functions within *SGAT* to determine appropriate zenith angles for each bird during the stationary breeding period when individuals are at known locations. To determine appropriate zenith angles at times of the year when the location is unknown (i.e. the nonbreeding season), we used the Hill-Ekstrom calibration method implemented using the function *findHEZenith* from the R package *TwGeos* (Lisovski et al. 2016). For each individual, we took a weighted median of all generated locations during the core of the wintering period (December and January) and used that centroid to define each individual's wintering location. Individuals were then assigned to one of the following four regions based on their estimated wintering centroid: northern Florida, southern Florida, the Bahamas, or Cuba (Supplemental Material Table S1).

Survival data for this analysis were collected from 1999 to 2005 as part of a separate study on the demography of eastern Painted Buntings (Sykes et al. 2019). Buntings were captured in mist nests situated at feeders filled with millet. Captured birds were immediately removed from mist nets, aged (hatch-year, second-year, or after-second-year), sexed, and banded. Birds were marked with 3 colored plastic leg bands and one U.S. Geological Survey (USGS) numbered aluminum leg band arranged 2 on each leg, in unique 4-band combinations for individual identification. Unbanded individuals were marked through 2003. In subsequent years, missing or faded color-bands were replaced on individuals still retaining the USGS metal bands, when

possible. Banded buntings were re-sighted at feeders during observation sessions starting in 2001. Observation sessions were conducted once annually during the breeding season at each site. In years when birds were banded (2001–2003), observation sessions were conducted at least one day before banding sessions. Feeders were arranged so all open feeding ports were visible by observers using 20–60× zoom spotting scopes, ~10 m away from the feeders (see Sykes et al. 2019 for further details). For this analysis, we included only data from males originally banded as adults (either second-year or after-second-year;  $n = 402$ ). We further included only banding locations within 20 km of our geocator deployment sites to ensure that survival estimates from the re-sight data corresponded as closely as possible to the geocator study (Supplemental Material Table S2).

Geocator recovery and CMR data were used to parameterize the integrated model. Mark re-sight data from individual feeders (Supplemental Material Table S2) were pooled to estimate a single survival probability for each region (North Carolina, South Carolina, Georgia, and Florida), forming the basis for implementing Equation (3) in this analysis. Thus, we did not model annual variation in survival and assumed that the time-averaged survival estimates from the mark-re-sight data are representative of the survival probabilities experienced by birds in the geocator study. Following Sykes et al. (2019), we included site-specific effects of human development within 700 m and feeder-level random effects on survival. We also included feeder-specific effort covariates in the detection model (Sykes et al. 2019). Using apparent survival estimates, we estimated weighted transition probabilities from each breeding region to each wintering region. To examine differences in biased and unbiased transition probabilities, we calculated unweighted (raw) transition probabilities by dividing the number of geolocators recovered at a breeding site from a single wintering region by the total number of geolocators recovered at a site from any wintering region. We used uninformative priors for all parameters. Posterior distributions were based on 3 chains, run for 20,000 iterations each after discarding the first 2,500 iterations as burn-in. Model convergence was assessed using R-hat values (Brooks and Gelman 1998) and by visual inspection of trace plots.

## RESULTS

### Simulation

Both  $\Psi$  and  $\phi_j$  were identifiable using the integrated model (Figure 1). As predicted, the correlation between relative nonbreeding survival and the bias in the uncorrected estimates of  $\Psi$  was positive (0.66), signifying that the transition probabilities for lowest-survival regions were

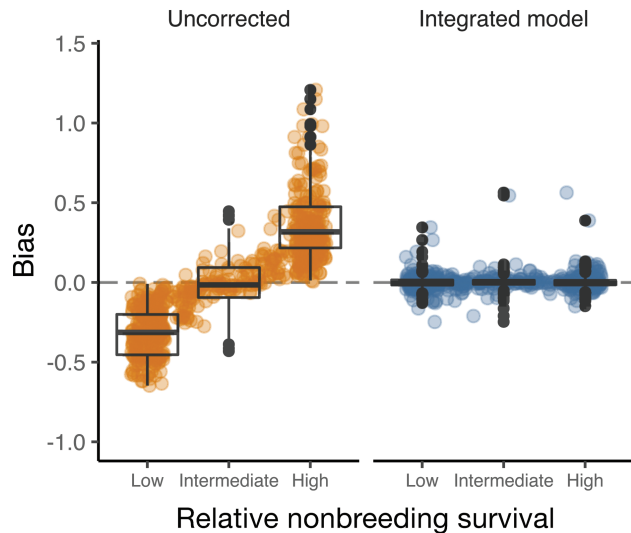


**FIGURE 1.** Bias in the estimated transition probabilities  $\Psi$  from 500 identifiability simulations. In each simulation, individuals migrate to one of three nonbreeding regions (ranked within each simulation as low, intermediate, or high), which differ in survival probability. Orange points show bias in the estimated transition probabilities as a function of relative survival (ranging from 0 to 1; see text for details) for each nonbreeding region based on the uncorrected geolocator recoveries. Blue points show bias for the same transition probabilities but estimated using the integrated model. Box-and-whisker plots summarize bias for nonbreeding regions categorized as the low, medium, or high survival region in each simulation, with the middle line showing the median, bottom and top hinges showing the 25th and 75th quantiles, and the top and bottom whiskers are 1.5 times the distance between the 25th and 75th quantiles. A small jitter has been added to aid visualization of the low and high survival points.

underestimated and overestimated for the highest-survival regions (Figure 1). This structural bias was substantial for the extreme low and high-survival regions, under- and over-estimating  $\Psi_j$  by nearly 45%, respectively. Transition probabilities to intermediate survival regions could be either overestimated or underestimated depending on whether survival was greater than or less than the average survival probability across all regions, respectively (Figure 1). In contrast, the integrated model returned unbiased estimates of  $\Psi$  regardless of the underlying survival probabilities (correlation =  $-0.03$ ), leading to the minimal relative bias of  $<1\%$  even at the most extreme low and high-survival sites (Figure 1). Estimates of  $\phi_j$  from the integrated model were also minimally biased ( $0.017$ ). Estimates of  $MC$  showed no bias when using the transition matrix from the integrated model (median relative bias  $<0.0001$ ) and a small negative bias for the uncorrected estimates (median relative bias =  $-0.04$ ). Although bias in  $MC_w$  was small on average, these estimates showed much larger variation than the  $MC_{\hat{\psi}}$  estimates (Figure 2). Root-mean-square error of

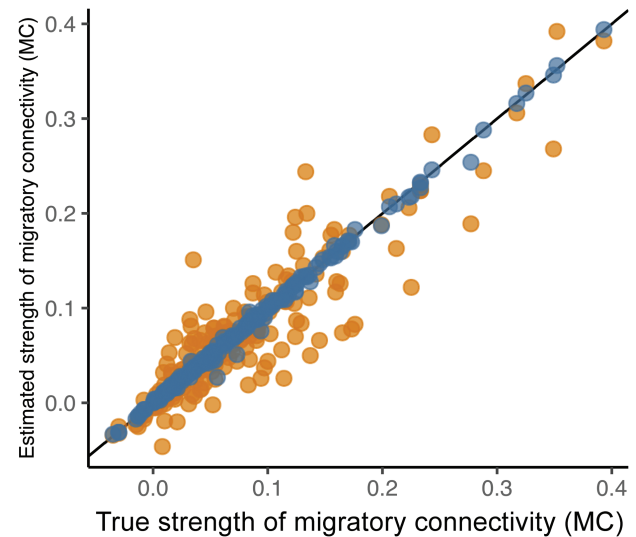


**FIGURE 2.** Relationship between the true and estimated strength of migratory connectivity ( $MC$ ) for the 500 identifiability simulations. Estimated  $MC$  are based on either the uncorrected transition probabilities (orange points) or the transition probabilities from the integrated model (blue points). The black line indicates a 1:1 relationship between the true and estimated  $MC$  values.

the  $MC_w$  estimates was  $0.03$ , nearly 10 times higher than the root-mean-square error of the  $MC_{\hat{\psi}}$  estimates ( $0.004$ ).

Estimability simulations indicated that, under more realistic sample sizes, some bias remains in the estimates of  $\Psi$  and  $\phi_j$  from the integrated model, though the integrated model greatly reduced bias in  $\Psi$  relative to the uncorrected estimates. Across all scenarios, the relative bias of  $\Psi_j$  for the extreme low and high-survival regions was generally  $<10\%$  for the integrated model, much lower than the approximately  $40\text{--}50\%$  of the uncorrected estimates. Even with only 10 geolocators deployed at each site and 75 individuals per year added to the capture–recapture data (Figure 3), the correlation between bias and nonbreeding survival was much lower in the integrated model ( $0.25$ ,  $0.23\text{--}0.27$ ) relative to the uncorrected estimates ( $0.63$ ,  $0.60\text{--}0.67$ ). Deploying additional geolocators reduced bias substantially, whereas adding additional individuals to the CMR data set had less influence on bias (Table 1). Bias in the integrated model generally decreased as both the length of the CMR study and the number of breeding sites and nonbreeding regions increased (see Supplemental Material Appendix S2), though the decreases in bias were small and the value of adding more years/sites generally decreased as more were added. Estimates of  $\phi_j$  were positively biased by approximately  $2\text{--}5\%$  under all estimability scenarios. Bias in  $\phi_j$  generally decreased as more marks (Table 1) and more years of CMR data were included in the analysis but

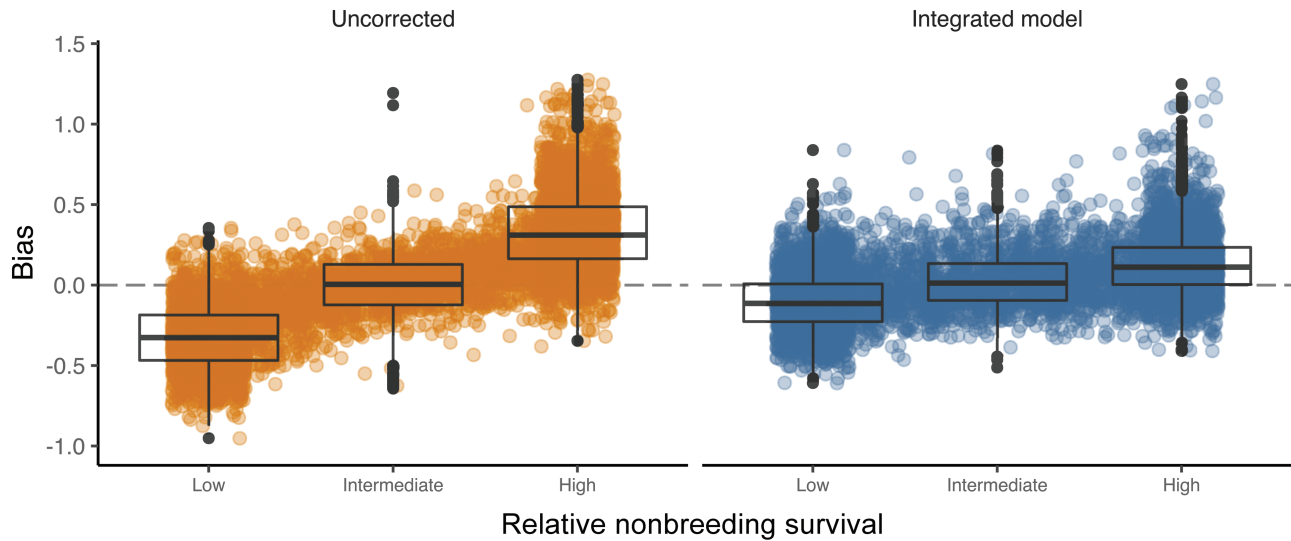


**FIGURE 3.** Bias in the estimated transition probabilities  $\Psi$  from 500 simulations in which 10 geolocators are deployed at each site and 75 marked individuals are added to the capture-recapture model in each year. In each simulation, individuals migrate to one of three nonbreeding regions (ranked within each simulation as low, intermediate, or high), which differ in survival probability. Orange points show bias in the estimated transition probabilities as a function of relative survival (ranging from 0 to 1; see text for details) for each nonbreeding region based on the uncorrected geocator recoveries. Blue points show bias for the same transition probabilities but estimated using the integrated model. Box-and-whisker plots summarize bias for nonbreeding regions categorized as the low, medium, or high survival region in each simulation, with the middle line showing the median, bottom and top hinges showing the 25th and 75th quantiles, and the top and bottom whiskers are 1.5 times the distance between the 25th and 75th quantiles. A small jitter has been added to aid visualization of the low and high survival points.

**TABLE 1.** Estimability of transition probabilities and nonbreeding survival probabilities as a function of the number of marks and geolocators deployed. Correlations are the mean and 95% confidence interval of the correlation between bias and relative nonbreeding survival across the 500 simulated data sets. The final column is the mean bias in the estimated survival probabilities for each nonbreeding region, denoted  $\phi_i$ .

Number of marks	Number of archival tags	Correlation-integrated model	Correlation-uncorrected	Bias in $\phi_i$
40	10	0.287 (0.264–0.310)	0.619 (0.591–0.647)	0.045
40	20	0.246 (0.225–0.268)	0.649 (0.625–0.673)	0.034
40	30	0.206 (0.186–0.226)	0.626 (0.604–0.648)	0.037
40	40	0.197 (0.177–0.217)	0.614 (0.593–0.634)	0.039
40	50	0.205 (0.185–0.225)	0.635 (0.615–0.655)	0.037
75	10	0.252 (0.229–0.274)	0.631 (0.603–0.659)	0.046
75	20	0.269 (0.249–0.290)	0.648 (0.624–0.672)	0.044
75	30	0.216 (0.196–0.236)	0.652 (0.628–0.675)	0.039
75	40	0.203 (0.182–0.224)	0.619 (0.598–0.639)	0.038
75	50	0.193 (0.173–0.213)	0.638 (0.618–0.659)	0.036
125	10	0.283 (0.261–0.305)	0.647 (0.618–0.676)	0.051
125	20	0.239 (0.217–0.261)	0.635 (0.611–0.660)	0.042
125	30	0.191 (0.172–0.211)	0.634 (0.613–0.656)	0.032
125	40	0.180 (0.160–0.199)	0.615 (0.594–0.636)	0.033
125	50	0.175 (0.156–0.194)	0.614 (0.593–0.634)	0.037
200	10	0.243 (0.221–0.264)	0.613 (0.584–0.642)	0.047
200	20	0.235 (0.214–0.256)	0.637 (0.614–0.660)	0.042
200	30	0.201 (0.181–0.221)	0.629 (0.608–0.651)	0.038
200	40	0.156 (0.137–0.176)	0.612 (0.591–0.633)	0.039
200	50	0.164 (0.145–0.183)	0.616 (0.596–0.636)	0.028
300	10	0.240 (0.217–0.263)	0.582 (0.554–0.610)	0.043
300	20	0.218 (0.198–0.238)	0.605 (0.581–0.629)	0.043
300	30	0.199 (0.179–0.219)	0.632 (0.610–0.653)	0.040
300	40	0.178 (0.158–0.198)	0.649 (0.628–0.670)	0.038
300	50	0.159 (0.139–0.178)	0.636 (0.616–0.657)	0.036



was not sensitive to the number of sites (Supplemental Material Appendix S2).

### Painted Bunting Survival and Migratory Connectivity

Estimates for apparent annual survival within breeding regions were similar for Florida (mean: 0.68, credible interval (CI): 0.58–0.76), Georgia (0.68, CI: 0.59–0.76), and South Carolina (0.66, CI: 0.58–0.74), but were notably lower in North Carolina (0.6, CI: 0.48–0.71). Of the 180 geolocators deployed in 2017 and 2018, we recovered 61 geolocators with usable data (Supplemental Material Table S1). Raw transition probabilities estimated from these geolocators suggested that Painted Buntings breeding in Florida was relatively evenly distributed among the 4 nonbreeding regions, birds from Georgia and South Carolina were most likely to winter in south Florida, and birds from North Carolina were most likely to winter in Cuba (Table 2). No geolocators were recovered in North Carolina from birds that had wintered in north or south Florida, and therefore transition probabilities to these wintering regions were estimated to be zero based on the raw recoveries.

Results from the integrated model suggest that the winter region affected annual survival. Survival was comparable for buntings wintering in north Florida (0.72, CI: 0.4–0.98), south Florida (0.75, CI: 0.49–0.98), and the Bahamas (0.72, CI: 0.39–0.98; Figure 4). Male buntings wintering in Cuba, however, had measurably lower annual survival probabilities (0.57, CI: 0.37–0.9). Due to regional survival variation in nonbreeding survival, transition probabilities from the integrated model differed from the raw estimates in important ways (Table 2). In particular, the integrated model suggested that birds breeding in Georgia and South Carolina breeding populations were less likely to winter in south Florida and more likely to winter in Cuba than suggested by the raw recovery data. These differences are consistent with over-estimation of connectivity to south Florida due to the high survival in that region and under-estimation of connectivity to Cuba due to the low survival there. For the North Carolina population, the integrated model actually indicated lower connectivity to Cuba than the raw data. This unintuitive result occurred because the integrated model estimated low but non-zero connectivity to north and south Florida despite no geolocator recoveries from these regions. In total, the estimated connectivity between North Carolina and Florida was approximately 15–20%, which more than offset differences between the integrated and raw connectivity estimates to Cuba.

### DISCUSSION

Our simulations confirm that estimating migratory transition probabilities from observed geolocator recoveries produces biased estimates when survival probabilities

**TABLE 2.** Transition probabilities from breeding sites to wintering sites, estimated from geolocators recovered on the breeding grounds in the 2017 and 2018 field seasons. Bolded values are the posterior mean of  $\Psi$  from the integrated models, with estimated 95% credible intervals in parentheses. Non-bolded values are the equivalent transition probabilities estimated from the raw recovery data. Note that the raw  $\Psi$  estimates are point estimates and do not provide any measure of uncertainty

Transition From	Transition to			
	N. Florida	S. Florida	Cuba	Bahamas
Florida	<b>0.245 (0.091–0.446)</b> 0.250	<b>0.202 (0.061–0.397)</b> 0.188	<b>0.264 (0.1–0.472)</b> 0.250	<b>0.289 (0.124–0.498)</b> 0.312
Georgia	<b>0.217 (0.074–0.417)</b> 0.211	<b>0.324 (0.152–0.536)</b> 0.368	<b>0.207 (0.06–0.409)</b> 0.158	<b>0.252 (0.098–0.459)</b> 0.263
S. Carolina	<b>0.269 (0.113–0.476)</b> 0.286	<b>0.327 (0.16–0.549)</b> 0.381	<b>0.281 (0.11–0.488)</b> 0.238	<b>0.123 (0.024–0.308)</b> 0.095
N. Carolina	<b>0.108 (0.003–0.442)</b> 0.000	<b>0.094 (0.002–0.363)</b> 0.000	<b>0.599 (0.22–0.874)</b> 0.800	<b>0.199 (0.023–0.557)</b> 0.200

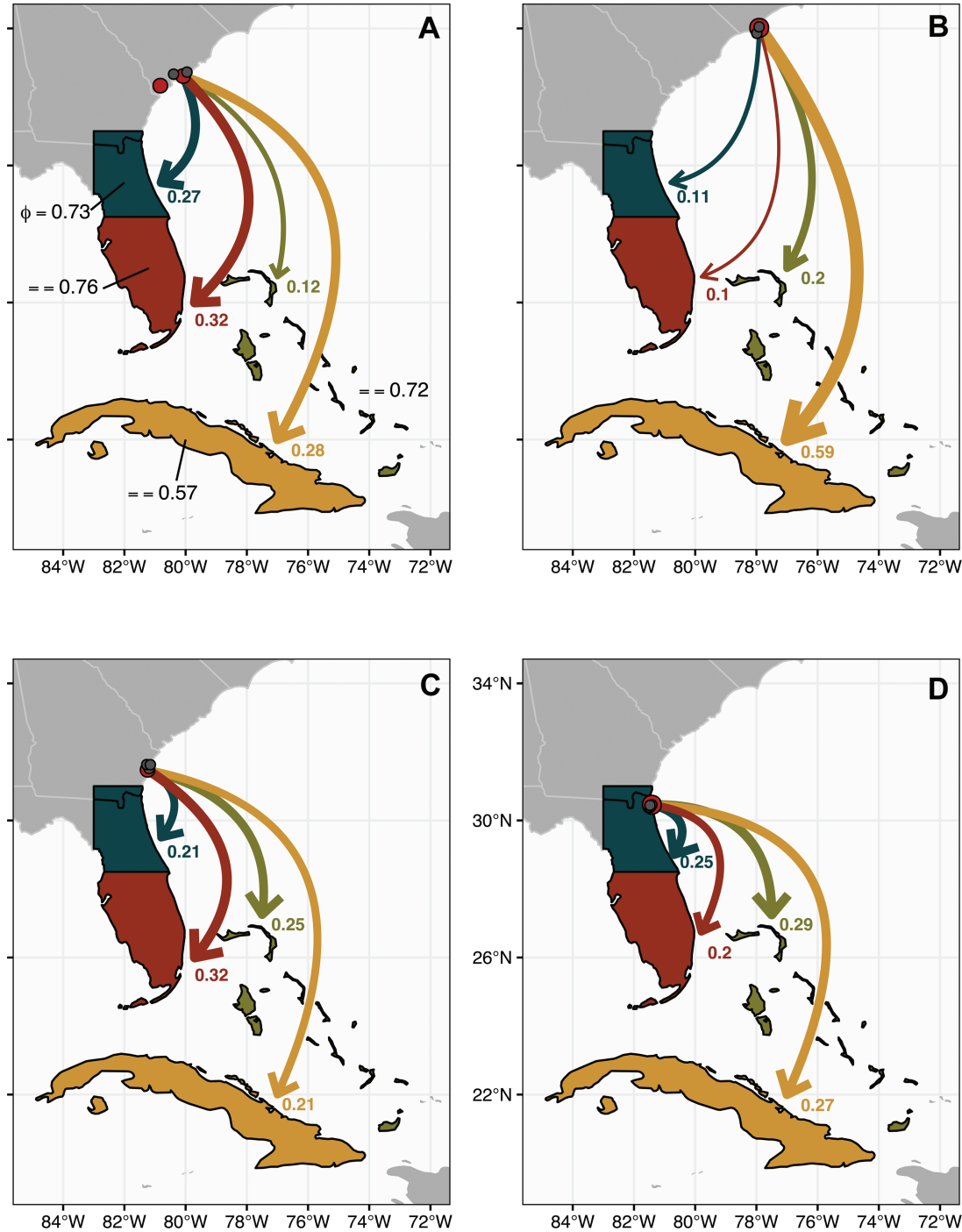


**FIGURE 4.** Estimated transition probabilities and nonbreeding survival of southeastern Painted Buntings (*Passerina ciris*) from (A) Kiawah Island and Spring Island, SC, (B) Wilmington, NC, (C) Little St. Simons Island, GA, and (D) Big Talbot Island State Park, FL. Red dots indicate geolocator deployment sites and grey dots indicate sites where mark–re-sight data were collected. Estimated survival probabilities for each of the four nonbreeding regions are shown in panel (A). Values at the base of each arrow are the estimated transition probabilities from the integrated model for each breeding site and nonbreeding region. Arrows are color-coded by nonbreeding region and sized relative to the estimated transition probabilities.

differ among nonbreeding regions. Given that regional variation in nonbreeding survival is the rule rather than the exception for most migratory species (Hewson et al.

2016, Healy et al. 2017, Kramer et al. 2018), survivorship bias is likely to be a pervasive issue for studies using archival tracking devices. As we demonstrate, the integration

of a probabilistic geolocator recovery model with mark-recapture data can reduce or eliminate survivorship bias, providing a practical approach for strengthening inferences about migratory connectivity.

The use of archival geolocators has grown dramatically over the past decade, with over 120 publications from 2010 to 2017 (McKinnon and Love 2018), motivating multiple research teams to investigate the effects of these geolocators on the survival of tracked individuals (Costantini and Møller 2013, Peterson et al. 2015, Brlik et al. 2020). However, we are not aware of any study that has been designed to account for survivorship bias on the interpretation of data from archival geolocators. Our results indicate that assuming observed geolocator recoveries accurately reflect the underlying migration patterns is potentially problematic and in extreme cases could lead to false inferences about which nonbreeding regions are most important for specific breeding populations. Reliance on raw recovery data may be especially problematic for archival tracking studies based on small sample sizes of deployed geolocators. Mortality or dispersal could result in no individuals being observed to migrate to certain nonbreeding regions. This was the case for our sample of Painted Buntings from North Carolina, which included no birds wintering in north or south Florida. In this case, the true transition probabilities are unlikely to be 0; instead, these zeros are probably the result of sampling variation with only a small number of tracked birds. Defining an explicit geolocator recovery model that treats the observed data as realizations of one or more stochastic process or sampling models provides a means to account for sampling variation and estimate the underlying process model parameters, even without integrating the survival data in the model.

Integrating geolocator recovery and survival data enables novel insights that neither source of information alone can provide. Our integrated model provided compelling evidence that survival probabilities of Painted Buntings wintering in Cuba may be 15–20% lower than for birds that winter in other parts of the range. Although the nonbreeding survival rates had high uncertainty, these results are consistent with the hypothesis that Painted Buntings migrating to Cuba face higher mortality than individuals wintering elsewhere in the range. One explanation for this result is that Painted Buntings in Cuba are at higher risk of capture as part of the illegal pet trade than birds that winter in Florida or the Bahamas. Reliable estimates of the number of buntings captured in Cuba or Florida are not available but anecdotal reports have documented localized trapping of as many as 700 buntings over 3 days in Cuba (Sykes Jr. et al. 2006, 2007). Additionally, of the 80 geolocators deployed in 2018 as part of this study, at least three are known to have been captured in Cuba and

Sykes et al. (2007) confirmed 19 buntings banded in the US and captured in Cuba. Of course, other explanations could explain our results, including longer migration distances required to reach Cuba or differences in habitat loss throughout the winter range. Our results nonetheless demonstrate how integrating tracking and survival data can lead to deeper insights about the dynamics of migratory species.

A common objective of recent tracking studies is to estimate the strength of migratory connectivity (Cohen et al. 2018), an index of the extent that individuals and populations remain together between seasons of the annual cycle. Even when the underlying transition probabilities are biased due to differential survival, our simulations indicate that *MC* is largely unbiased when derived from observed geolocator recoveries. This result is not unexpected because the *MC* metric is based on the relative links between breeding and nonbreeding populations, rather than the absolute transition probabilities. In other words, transition probabilities to low-survival nonbreeding regions, estimated from the raw recoveries, will be underestimated for all breeding sites and as a result, the correlation of distances between breeding and nonbreeding populations will remain unbiased. These results suggest that, on average, published estimates of *MC* based on archival geolocators should be considered unbiased. However, we found that *MC* estimates based on the integrated model were, on average, more precise, that is much closer to the true *MC* value, than estimates based on raw recovery data. This result is likely due to explicitly accounting for process and sampling uncertainty in the geolocator recovery model. By viewing the realized recoveries as stochastic processes, the integrated model attempts to separate the expected transition and survival probabilities from the process and sampling noise inherent to the data collection process. Reducing the influence of sampling and process uncertainty in the  $\Psi$  estimates in turn reduces noise in the estimates of *MC* compared to estimates based on the raw geolocator recoveries. Future work that allows researchers to directly account for survivorship bias and produce more accurate estimates of *MC* would be beneficial.

Our integrated approach permits unbiased estimates of nonbreeding survival and transition probabilities for seasonal ranges, but makes several assumptions. First, we assume that nonbreeding survival is independent of breeding origin. If nonbreeding survival differs among breeding sites, because for example, individuals migrate different distances, then site-specific transition probabilities will be confounded with variation in site-specific nonbreeding survival. Second, we assume that geolocator recovery probability is independent of nonbreeding location. If the probability of recovering geolocators (conditional on an

individual surviving and returning to the deployment site) is influenced by events outside the breeding season, this heterogeneity would incorrectly be interpreted as heterogeneity in survival. Third, individuals tracked using archival geolocators are assumed to have the same survival probability as individuals in the capture–recapture data set. Recent meta-analyses of light-level geocator studies found that these geolocators can have a small, negative effect on survival, especially for small and highly aerial species (Costantini and Møller 2013, Brlik et al. 2020). However, geocator effects should not bias transition probability estimates as long as they are independent of where individuals overwinter. In this case, the lower return rate of geocator individuals will be reflected in lower geocator recovery probabilities but other parameters should be unbiased. Fourth, integrating geocator recovery and capture–recapture models assumes independence of the two data sets. Strictly speaking, if some individuals are shared between the two data sets, variance parameters in the model will be underestimated, though small violations of this assumption are unlikely to affect inference (Abadi et al. 2010). Fifth, we assumed no uncertainty in the nonbreeding region of each tracked individual. Some archival geolocators, particularly light-level geolocators, have substantial uncertainty and even with large nonbreeding regions, some individuals may not be assigned to regions with 100% accuracy. Uncertainty in nonbreeding regions could be incorporated into the analysis by treating nonbreeding assignments as categorical random variables with probabilities estimated from the raw tracking data, though this modification is beyond the scope of this paper. Finally, assumptions of the chosen survival model also apply to the integrated geocator recovery model.

Prior to the development of miniaturized archival tracking devices, migratory animals could not be tracked across their entire annual cycle. This technology has created novel research opportunities for thousands of species, but data from archival geolocators must be carefully interpreted. Discussions about inferences from archival geolocators have mainly focused on whether geolocators influence the fitness or behavior of tracked individuals (Arlt et al. 2013, Costantini and Møller 2013, Brlik et al. 2020). Although these issues are important, the effects of survivorship bias on inference from archival geolocators have not been widely acknowledged. Our results demonstrate that survivorship bias, a potentially ubiquitous outcome of archival geolocators, can be reduced or eliminated if data for estimating survival is also available for each deployment site. Thanks to the focus on quantifying geocator effects, many tracking studies are likely already collecting mark–recapture or mark–re-sight data that could be used to fit the integrated model presented here. In cases where researchers are designing new tracking

studies, the collection of these auxiliary survival data should be prioritized both to measure geocator effects and obtain accurate transition probabilities and regional nonbreeding survival probabilities. Although estimation of MC appears to be relatively robust to variation in survival, transition probabilities are not. Given that little is known about regional survival in most species, inferences about migration patterns from archival patterns should be interpreted very cautiously unless measures are taken to correct for survivorship bias. Improving inferences from archival geolocators through proper data collection and further development of integrated models will enable this technology to further transform the study of small, migratory organisms.

## SUPPLEMENTAL MATERIAL

Supplemental material is available online at *Ornithological Applications* online.

## ACKNOWLEDGMENTS

We thank the many volunteers who maintained feeders and reported Painted Bunting encounters, and the Spring Island Trust, Bald Head Island Conservancy, Little St. Simons Island, and North Florida Land Trust for providing housing and support during geocator deployment and recovery. Thanks to J.A. Royle, J. Sauer, S. Schirmer, and one anonymous reviewer for comments that improved earlier drafts of this paper, particularly S. Schirmer for providing the proof found in [Supplemental Material Appendix S1](#).

**Funding statement:** This work was supported by a Neotropical Migratory Bird Protection Act grant (#6759) from the U.S. Fish & Wildlife Service and by funding from the Disney Conservation Fund, the Spring Island Land Trust, the Cornell Lab of Ornithology, the Smithsonian Institution, and Utah State University. Use of trade, product, or firm names does not imply endorsement by the U.S. Government.

**Ethics statement:** All research activities were performed under protocols approved by the animal care and use committees of the authors' institutions, permitted by the relevant federal and state authorities, and in compliance with the Guidelines to the Use of Wild Birds in Research (Fair et al. 2010).

**Author contributions:** C.S.R. conceived the study and conducted simulations. C.S.R., A.J.S., V.R.G., A.M.G., and T.S.S. designed and conducted the geocator study. P.W.S. and M.C.F. designed and carried out the mark–re-sight study. A.J.S. analyzed the geocator data and A.V.T. produced the integrated analysis. C.S.R., V.R.G., M.C.F., P.W.S., and T.S.S. acquired funding. C.S.R., A.J.S., and A.V.T. wrote the first version of the manuscript and all authors contributed to subsequent revisions.

**Data availability:** Analyses reported in this article can be reproduced using the data provided by [Rushing et al. \(2021\)](#).



## LITERATURE CITED

- Abadi, F., O. Gimenez, R. Arlettaz, and M. Schaub (2010). An assessment of integrated population models: Bias, accuracy, and violation of the assumption of independence. *Ecology* 91:7–14.
- Arlt, D., M. Low and T. Pärt (2013). Effect of geolocators on migration and subsequent breeding performance of a long-distance passerine migrant. *PLoS One* 8:e82316.
- Auger-Méthé, M., C. Field, C. M. Albertsen, A. E. Derocher, M. A. Lewis, I. D. Jonsen, and J. Mills Flemming (2016). State-space models' dirty little secrets: Even simple linear Gaussian models can have estimation problems. *Scientific Reports* 6:26677.
- Brlík, V., J. Koleček, M. Burgess, S. Hahn, D. Humple, M. Krist, J. Ouwehand, E. L. Weiser, P. Adamík, J. A. Alves, et al. (2020). Weak effects of geolocators on small birds: A meta-analysis controlled for phylogeny and publication bias. *The Journal of Animal Ecology* 89:207–220.
- Brooks, S. P., and A. Gelman (1998). General methods for monitoring convergence of iterative simulations. *Journal of Computational and Graphical Statistics* 7:434–455.
- Brownie, C., J. E. Hines, J. D. Nichols, K. H. Pollock, and J. B. Hestbeck (1993). Capture–recapture studies for multiple strata including non-Markovian transitions. *Biometrics* 49:1173–1187.
- Cohen, E. B., J. A. Hostetler, M. T. Hallworth, C. S. Rushing, T. S. Sillett, and P. P. Marra (2018). Quantifying the strength of migratory connectivity. *Methods in Ecology and Evolution* 9:513–524.
- Cohen, E. B., J. A. Hostetler, J. A. Royle, and P. P. Marra (2014). Estimating migratory connectivity of birds when re-encounter probabilities are heterogeneous. *Ecology and Evolution* 4:1659–1670.
- Cooper, N. W., D. N. Ewert, J. M. Wunderle Jr, E. H. Helmer, and P. P. Marra (2019). Revising the wintering distribution and habitat use of the Kirtland's Warbler using playback surveys, citizen scientists, and geolocators. *Endangered Species Research* 38:79–89.
- Costantini, D., and A. P. Møller (2013). A meta-analysis of the effects of geolocator application on birds. *Current Zoology* 59:697–706.
- Delmore, K. E., J. W. Fox, and D. E. Irwin (2012). Dramatic intra-specific differences in migratory routes, stopover sites and wintering areas, revealed using light-level geolocators. *Proceedings. Biological Sciences* 279:4582–4589.
- Domeier, M. L., and N. Nasby-Lucas (2013). Two-year migration of adult female white sharks (*Carcharodon carcharias*) reveals widely separated nursery areas and conservation concerns. *Animal Biotelemetry* 1:2.
- Eckert, S. A., and B. S. Stewart (2001). Telemetry and satellite tracking of whale sharks, *Rhincodon typus*, in the Sea of Cortez, Mexico, and the north Pacific Ocean. Pages 299–308. In *The Behavior and Sensory Biology of Elasmobranch Fishes: An Anthology in Memory of Donald Richard Nelson* (E. K. Balon, T. C. Tricas and S. H. Gruber, Editors). Springer Netherlands, Dordrecht, The Netherlands.
- Fair, J., E. Paul, and J. Jones (Editors) (2010). *Guidelines to the Use of Wild Birds in Research*. Ornithological Council. Washington, D.C., USA.
- Fraser, K. C., B. J. Stutchbury, C. Silverio, P. M. Kramer, J. Barrow, D. Newstead, N. Mickle, B. F. Cousens, J. C. Lee, D. M. Morrison, et al. (2012). Continent-wide tracking to determine migratory connectivity and tropical habitat associations of a declining aerial insectivore. *Proceedings of the Royal Society B* 279:4901–4906.
- Gimenez, O., A. Viallefont, E. A. Catchpole, R. Choquet, and B. J. Morgan (2004). Methods for investigating parameter redundancy. *Animal Biodiversity and Conservation* 27:561–572.
- Hallworth, M. T., and P. P. Marra (2015). Miniaturized GPS tags identify non-breeding territories of a small breeding migratory songbird. *Scientific Reports* 5:11069.
- Healy, S. J., S. G. Hinch, A. D. Porter, E. L. Rechisky, D. W. Welch, E. J. Eliason, A. G. Lotto, and N. B. Furey (2017). Route-specific movements and survival during early marine migration of hatchery steelhead *Oncorhynchus mykiss* smolts in coastal British Columbia. *Marine Ecology Progress Series* 577:131–147.
- Herr, C. A., P. W. Sykes, and J. Klicka (2011). Phylogeography of a vanishing North American songbird: The Painted Bunting (*Passerina ciris*). *Conservation Genetics* 12:1395–1410.
- Hewson, C. M., K. Thorup, J. W. Pearce-Higgins, and P. W. Atkinson (2016). Population decline is linked to migration route in the Common Cuckoo. *Nature Communications* 7:12296.
- Hostetler, J. A., and M. T. Hallworth (2018). MigConnectivity: Estimate strength of migratory connectivity for migratory animals. R Package Version 0.3.0. <https://rdr.io/github/SMBC-NZP/MigConnectivity/>
- Jiménez López, M. E., D. M. Palacios, A. Jaramillo Legorreta, J. Urbán R, and B. R. Mate (2019). Fin whale movements in the Gulf of California, Mexico, from satellite telemetry. *PLoS One* 14:e0209324.
- Kellner, K. (2016). JagsUI: A Wrapper Around Rjags to Streamline JAGS Analyses. R Package v. 1.4.2. <https://github.com/kenkellner/jagsUI>
- Korner-Nievergelt, F., C. Prévot, S. Hahn, L. Jenni, and F. Liechti (2017). The integration of mark re-encounter and tracking data to quantify migratory connectivity. *Ecological Modelling* 344:87–94.
- Korner-Nievergelt, F., A. Sauter, P. W. Atkinson, J. Guélat, W. Kania, M. Kéry, U. Köppen, R. A. Robinson, M. Schaub, K. Thorup, H. V. D. Jeugd, and A. J. V. Noordwijk (2010). Improving the analysis of movement data from marked individuals through explicit estimation of observer heterogeneity. *Journal of Avian Biology* 41:8–17.
- Kramer, G. R., D. E. Andersen, D. A. Buehler, P. B. Wood, S. M. Peterson, J. A. Lehman, K. R. Aldinger, L. P. Bulluck, S. Harding, J. A. Jones, et al. (2018). Population trends in Vermivora warblers are linked to strong migratory connectivity. *Proceedings of the National Academy of Sciences USA* 115:E3192–E3200.
- Lisovski, S., S. Bauer, M. Briedis, S. C. Davidson, K. L. Dhanjal-Adams, M. T. Hallworth, J. Karagicheva, C. M. Meier, B. Merkel, J. Ouwehand, et al. (2020). Light-level geolocator analyses: A user's guide. *Journal of Animal Ecology* 89:221–236.
- Lisovski, S., and S. Hahn (2012). GeoLight—processing and analysing light-based geolocator data in R. *Methods in Ecology and Evolution* 3:1055–1059.
- Lisovski, S., S. Wotherspoon, and M. Sumner (2016). TwGeos: Basic Data processing for light-level geolocation archival tags. R Package v 0.1.2. <https://github.com/SWotherspoon/BAStag>
- McKinnon, E. A., and O. P. Love (2018). Ten years tracking the migrations of small landbirds: Lessons learned in the golden age of bio-logging. *The Auk: Ornithological Advances* 135:834–856.
- Naidoo, R., M. J. Chase, P. Beytell, P. Du Preez, K. Landen, G. Stuart-Hill, and R. Taylor (2016). A newly discovered wildlife migration in Namibia and Botswana is the longest in Africa. *Oryx* 50:138–146.

- Nichols, J. D., R. E. Reynolds, R. J. Blohm, R. E. Trost, J. E. Hines, and J. P. Bladen (1995). Geographic variation in band reporting rates for Mallards based on reward banding. *The Journal of Wildlife Management* 59:697–708.
- Peterson, S. M., H. M. Streby, G. R. Kramer, J. A. Lehman, D. A. Buehler, and D. E. Andersen (2015). Geolocators on Golden-winged Warblers do not affect migratory ecology. *The Condor: Ornithological Applications* 117:256–261.
- Plummer, M. (2012). JAGS: Just Another Gibbs Sampler, version 3.3.0. <http://mcmc-jags.sourceforge.net/>
- R Core Team (2016). R: A Language and Environment for Statistical Computing. R Foundation for Statistical Computing, Vienna, Austria. <http://www.r-project.org/>
- Rappole, J. H., and A. R. Tipton (1991). New harness design for attachment of radio transmitters to small passerines. *Journal of Field Ornithology* 62:335–337.
- Richter, H. V., and G. S. Cumming (2008). First application of satellite telemetry to track African straw-coloured fruit bat migration. *Journal of Zoology* 275:172–176.
- Ruegg, K. C., E. C. Anderson, K. L. Paxton, V. Apkenas, S. Lao, R. B. Siegel, D. F. DeSante, F. Moore, and T. B. Smith (2014). Mapping migration in a songbird using high-resolution genetic markers. *Molecular Ecology* 23:5726–5739.
- Rushing, C. S., T. B. Ryder, A. L. Scarpignato, J. F. Saracco, and P. P. Marra (2016). Using demographic attributes from long-term monitoring data to delineate natural population structure. *Journal of Applied Ecology* 53:491–500.
- Rushing, C. S., A. M. Van Tatenhove, A. Sharp, V. Ruiz-Gutierrez, M. C. Freeman, P. W. Sykes Jr., A. M. Given, and T. S. Sillett (2021). Data from: Integrating tracking and resight data enables unbiased inferences about migratory connectivity and winter range survival from archival tags. *Ornithological Applications* 123:1–14. <https://doi.org/10.5061/dryad.5mkkwh75d>
- Sæther, B. E. (1989). Survival rates in relation to body weight in European birds. *Ornis Scandinavica* 20:13–21.
- Sawyer, H., M. J. Kauffman, R. M. Nielson, and J. S. Horne. (2009). Identifying and prioritizing ungulate migration routes for landscape-level conservation. *Ecological Applications* 19:2016–2025.
- Scarpignato, A. L., A. L. Harrison, D. J. Newstead, L. J. Niles, R. R. Porter, M. van den Tillaart, and P. P. Marra (2016). Field-testing a new miniaturized GPS-Argos satellite transmitter (3.5 g) on migratory shorebirds. *Wader Study* 123. <https://www.waderstudygroup.org/article/8782/>
- Smith, M., M. Bolton, D. J. Okill, R. W. Summers, P. Ellis, F. Liechti, and J. D. Wilson (2014). Geolocator tagging reveals Pacific migration of Red-necked Phalarope *Phalaropus lobatus* breeding in Scotland. *Ibis* 156:870–873.
- Sykes, P. W., M. C. Freeman, J. J. Sykes, J. T. Seginak, M. D. Oleyar, and J. P. Egan (2019). Annual survival, site fidelity, and longevity in the eastern coastal population of the Painted Bunting (*Passerina ciris*). *The Wilson Journal of Ornithology* 131:96–110.
- Sykes, P. W. Jr., and S. Holzman (2005). Current range of the eastern population of Painted Bunting (*Passerina ciris*). Part 1: Breeding. *North American Birds* 59:14.
- Sykes, P. W., S. Holzman, and E. E. Iñigo-Elias (2007). Current range of the eastern population of Painted Bunting (*Passerina ciris*). Part II: winter range. *North American Birds* 61:29.
- Sykes, P. W. Jr., L. Manfredi, and M. Padura (2006). A brief report on the illegal cage-bird trade in southern Florida: A potentially serious negative impact on the eastern population of Painted Bunting (*Passerina ciris*). *North American Birds* 60:4.